MASS-BALANCE APPROACH TO SEGMENTATION OF WATER DISTRIBUTION IN SOIL PORES

Andrey Guber and Alexandra Kravchenko

Michigan State University, East Lansing, MI

MICHIGAN STATE UNIVERSITY

Pedofract IX International Workshop on Advances in Soil Scaling: Theories, Techniques and Applications, El Barco de Avila (Spain), July 9-12, 2019

Outline of the talk

I. Need for improvement of X-ray CT segmentation methods

II. Single-and dual-energy CT with monochromatic synchrotron X-rays

III. Mass-balance approach to segmentation

IV. Tests and validation

V. Applications

I. Need for improvement of X-ray CT segmentation methods

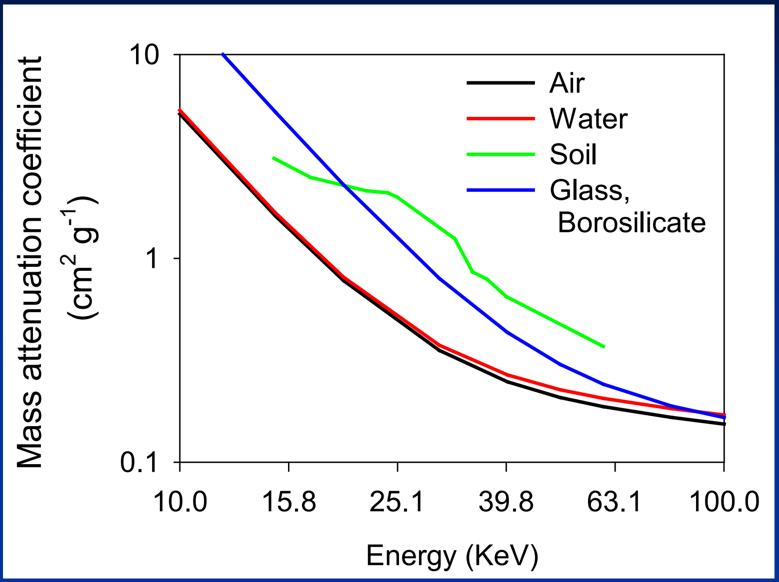

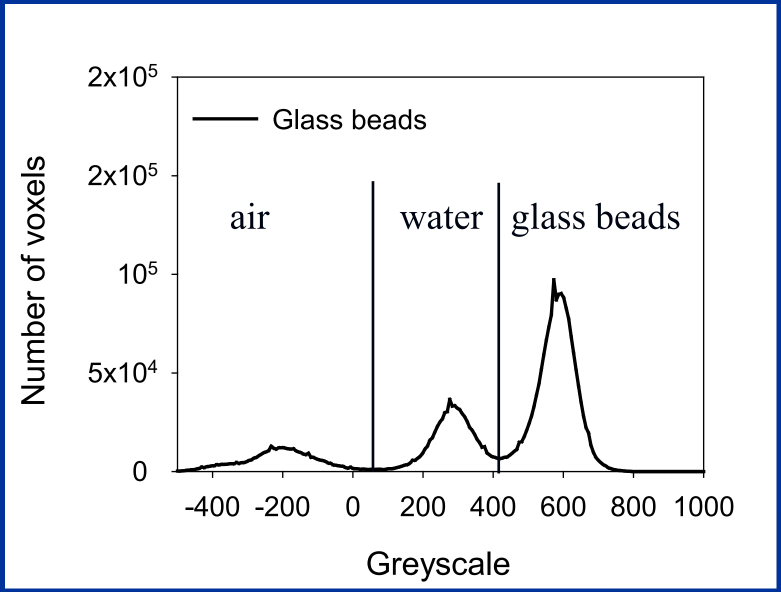

Borosilicate glass beads with water and air

Original image

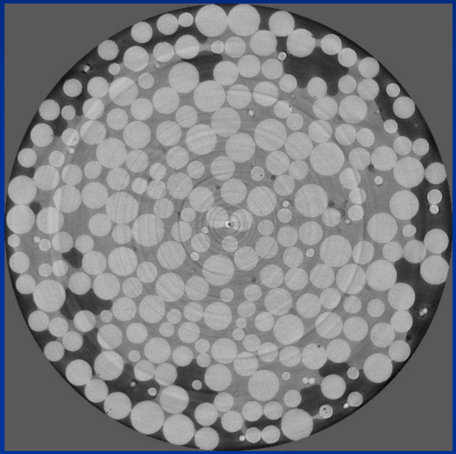

Water (black)

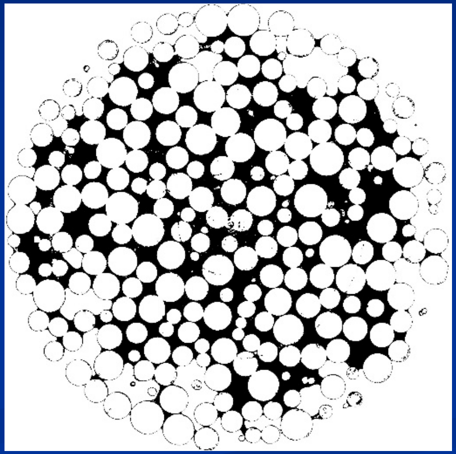

Solid (black)

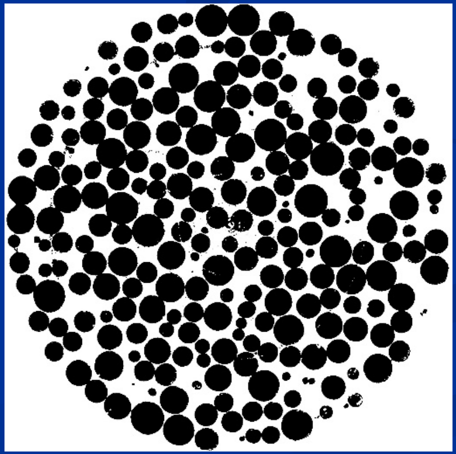

Air (white)

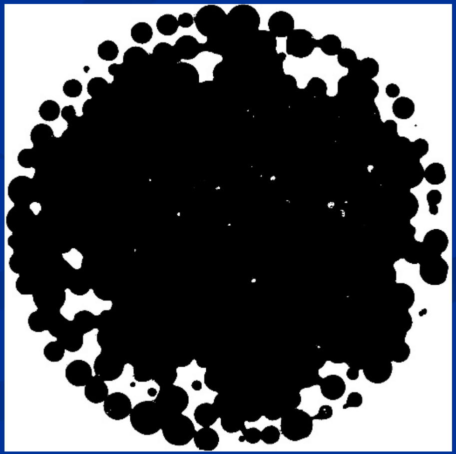

I. Need for improvement of X-ray CT segmentation methods

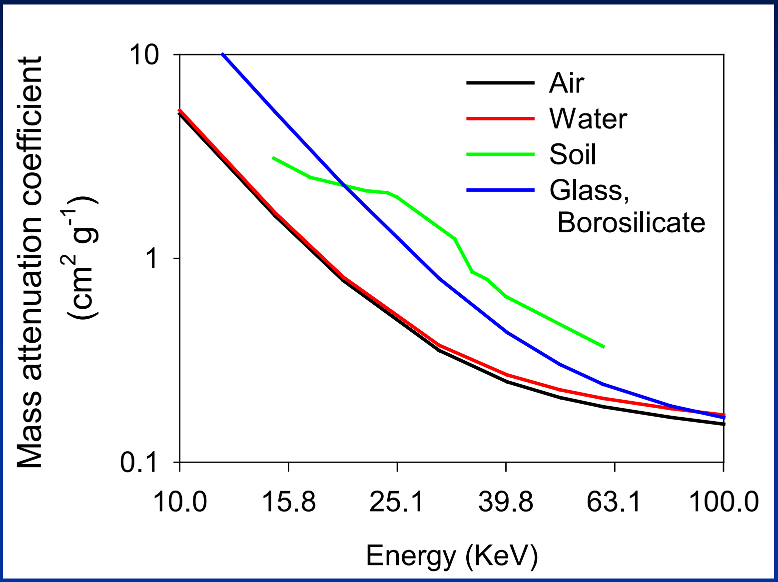

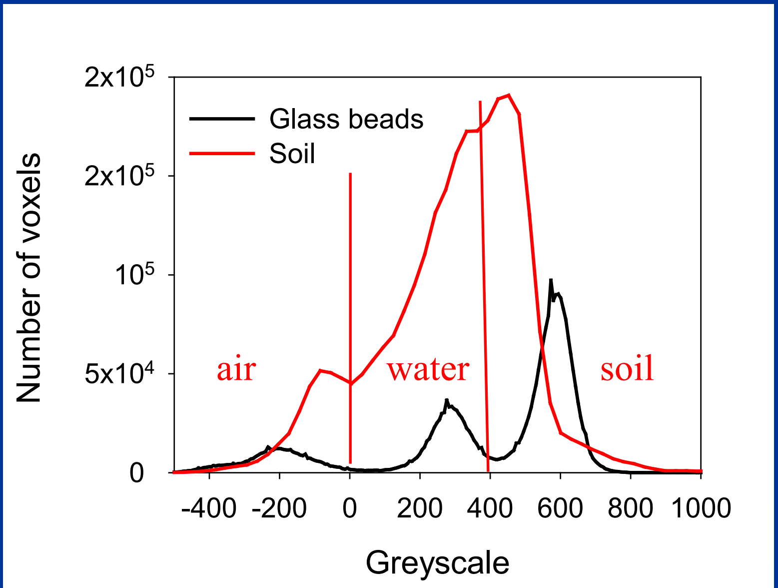

Soil with water and air

Original image

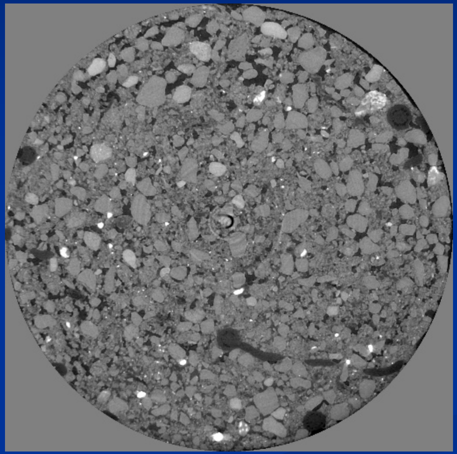

Water (black)

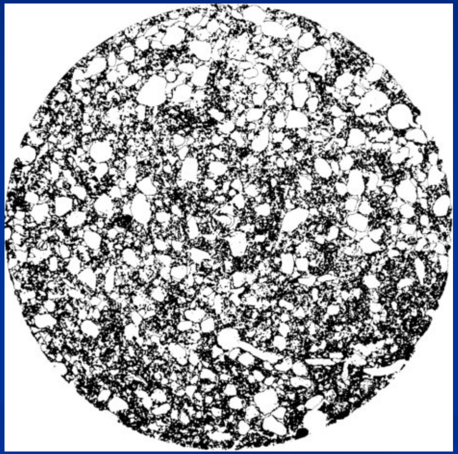

Solid (black)

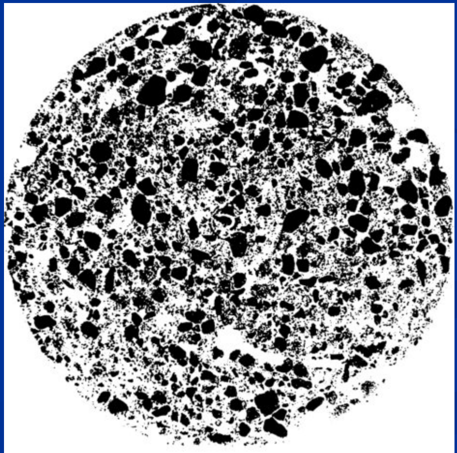

Air (white)

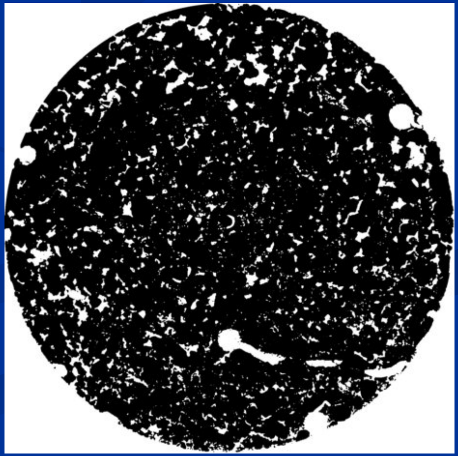

I. Need for improvement of X-ray CT segmentation methods

1. Segmentation in undisturbed soils is challenging, because the shape of grayscale histograms is often unimodal.

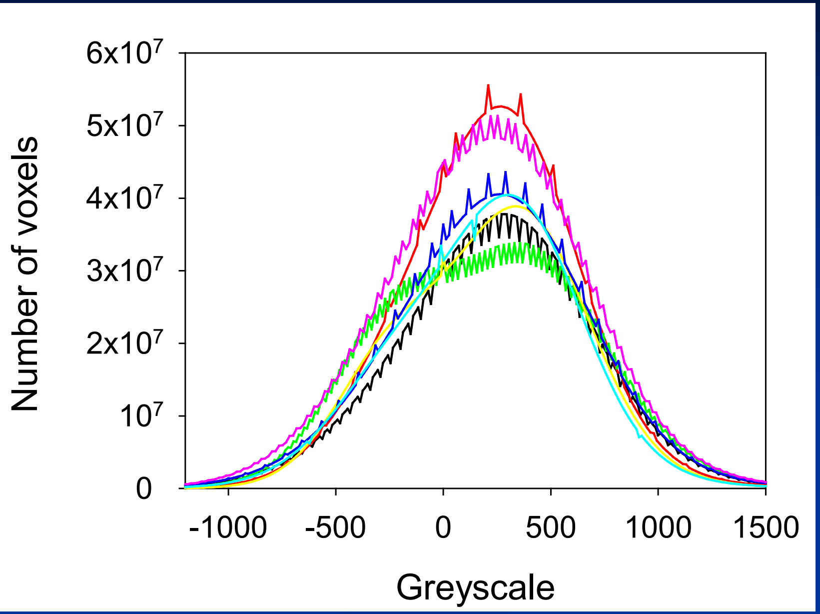

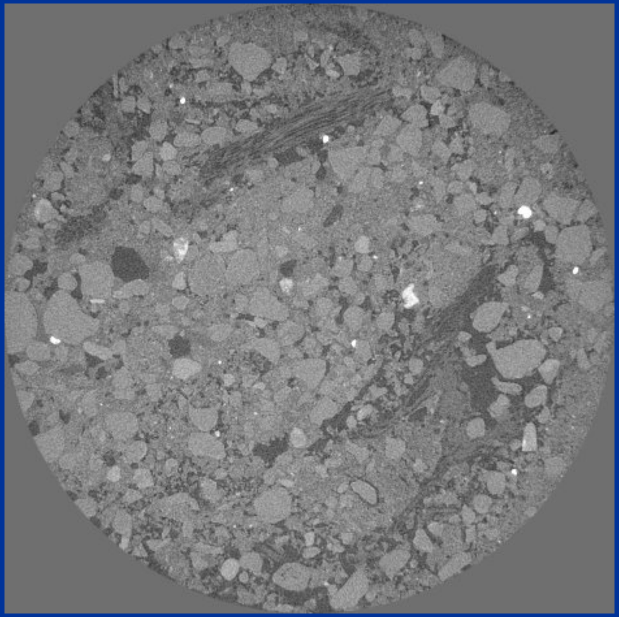

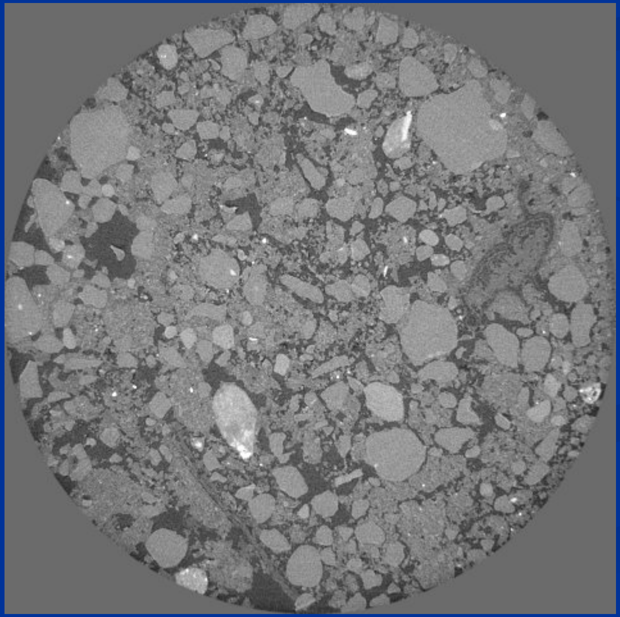

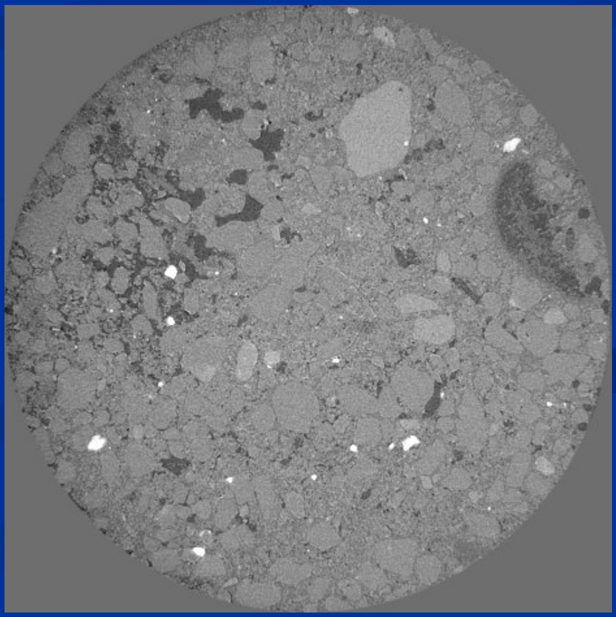

I. Need for improvement of X-ray CT segmentation methods

2. Partial volume effect:

- Due to limitations in scanning resolutions, voxel size (4-100 μm) is larger than the size of most soil pores.
- Each voxel consists of different fractions of solid, liquid and air (partial volume effect).
- Current methods of segmentation assign a single phase (solid, liquid or air) to each voxel, and typically underestimate volumes of liquid and air phases.
- **Solution: to develop a procedure for calculation of each fraction in X-ray CT voxels.**

single voxel

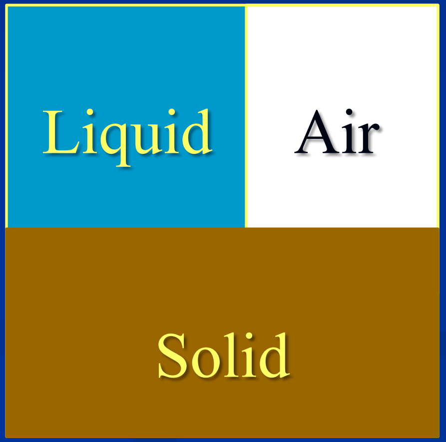

II. Single-and dual-energy CT with monochromatic synchrotron X-rays

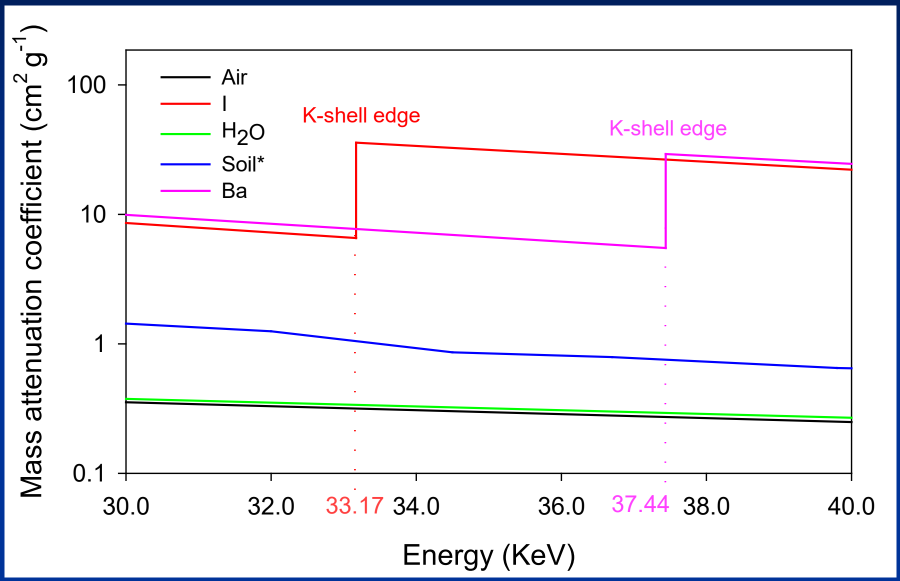

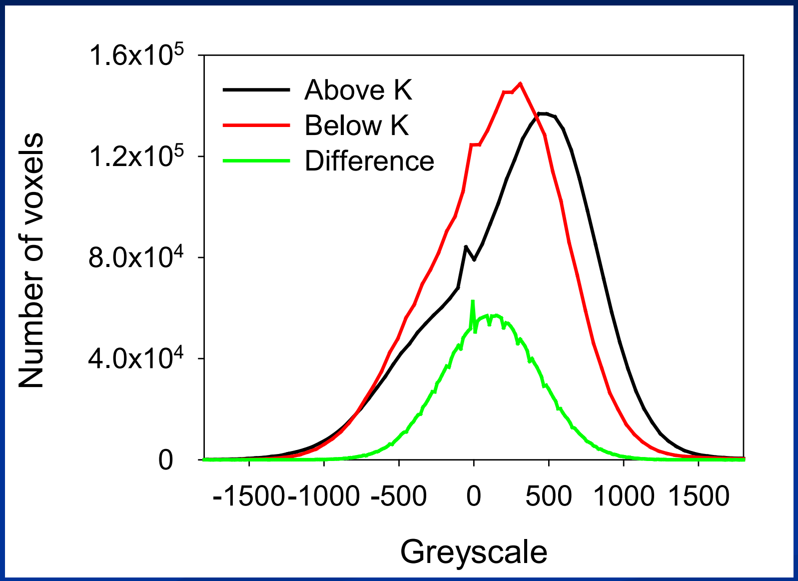

above K-edge

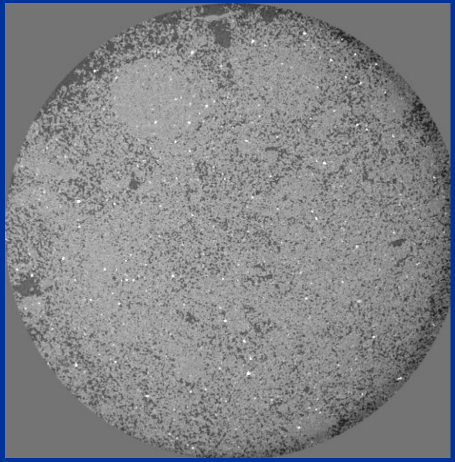

below K-edge

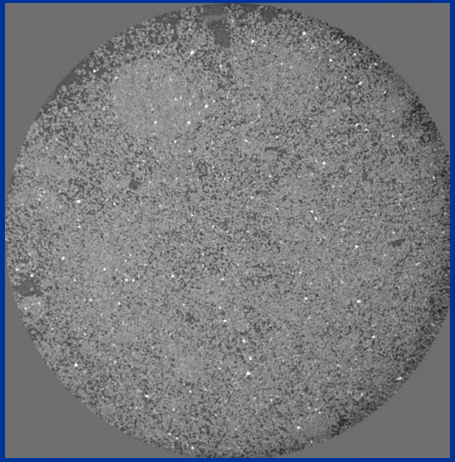

difference

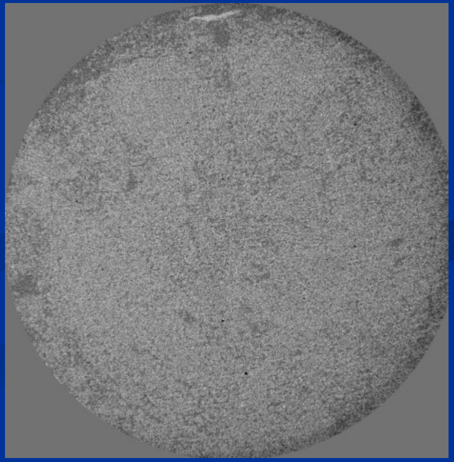

III. Mass-balance approach to segmentation.

The greyscale values G_i of a material at energy level i :

$$G_i = \mu_i r F \qquad (1)$$

μ_i is the liner attenuation coefficient of material at energy level i [cm^{-1}];

r is the scanning resolution (voxel sixe) [cm];

F is the scaling factor equal 10^{-6} [-];

For the soil with applied dopant solution and scanned at energies below (G_b) and above (G_a) the K-shell edge subtraction the two images gives:

$$\Delta G = rF\Delta\mu^I C_{I\,j}; \qquad C_{I\,j} = \phi_j S_{I\,j}; \qquad \Delta\mu^I = \mu_a^I - \mu_b^I \qquad (2)$$

μ_a^I and μ_b^I are the mass attenuation coefficients for the dopant at energies above and below K-shell edge [$cm^2\ g^{-1}$]

$S_{I\,j}$ is the concentration of the dopant in soil pores [$g\ cm^{-3}$]

ϕ_j is the porosity of j-voxel filled by the dopant solution [$cm^3 cm^{-3}$]

Sum of greyscale values in voxels:

$$\sum_{j=1}^{n} \Delta G_j = rF\Delta\mu^I \sum_{j=1}^{n} \phi_j\, C_{I\,j} = rF\Delta\mu^I N S_w C_{I\,w} \qquad (3)$$

n is the total number of voxels with the dopant solution [-]

N is the total number of voxels in the scanned sample [-]

S_w is the volumetric content of the applied solution in soil [$cm^3 cm^{-3}$]

$C_{I\,w}$ is the concentration of the dopant in the applied solution [$g\ cm^{-3}$]

III. Mass-balance approach to segmentation.

1. Estimating G^* using cumulative ΣΔG for reversed greyscale values and applied mass of the dopant :

$$\sum_{j=1}^{n} \Delta G_j = rF\Delta\mu^I N S_w C_{I\,w}$$

2. For each voxel calculating volumetric fraction filled by the dopant solution:

$$Sw_j = 0; \qquad G_j < G^*$$

$$Sw_j = G_j/(rF\Delta\mu^I C_{I\,j}); \qquad G_j > G^*$$

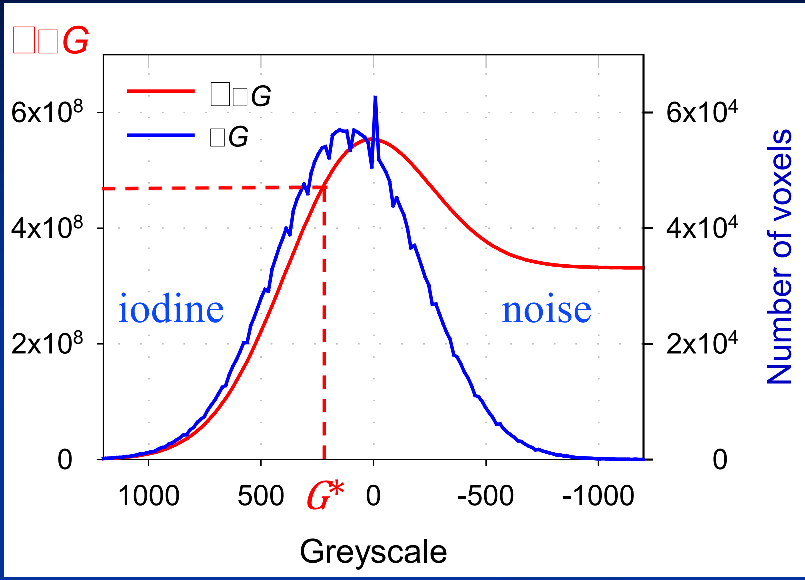

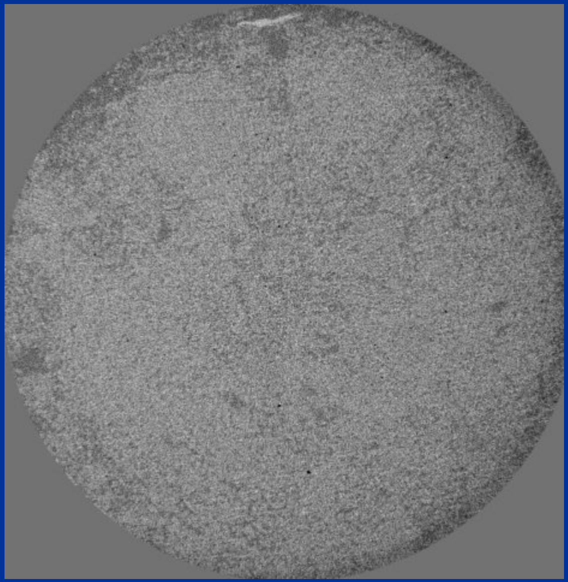

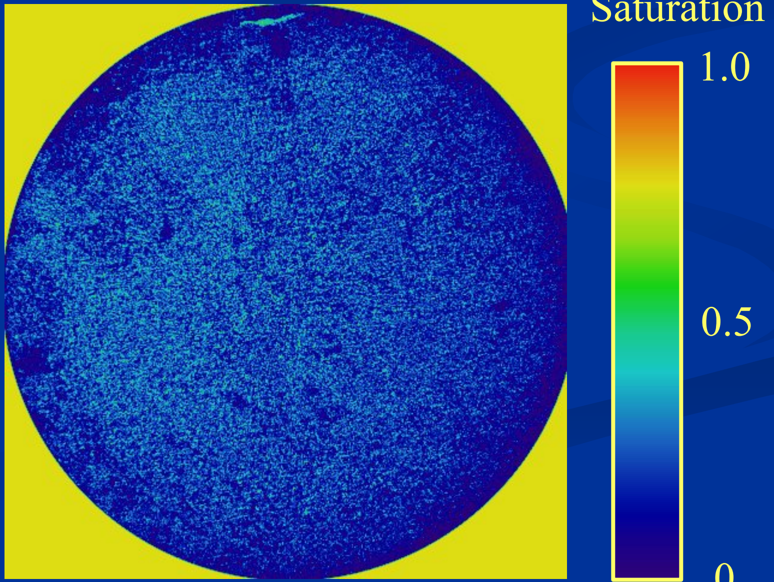

IV. Tests and validation

Histograms obtained using triple-energy X-ray CT for 10% solutions of KI and $BaCl_2$, and dry soil free of I and Ba.

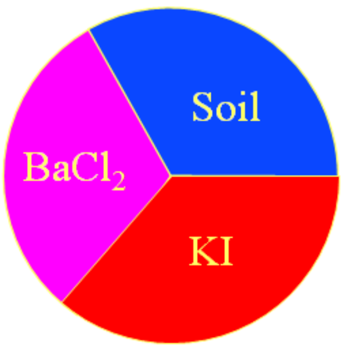

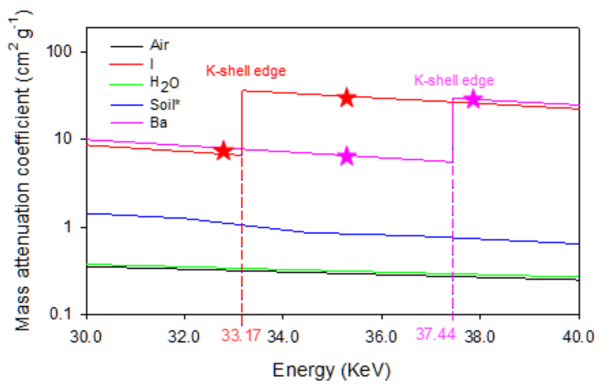

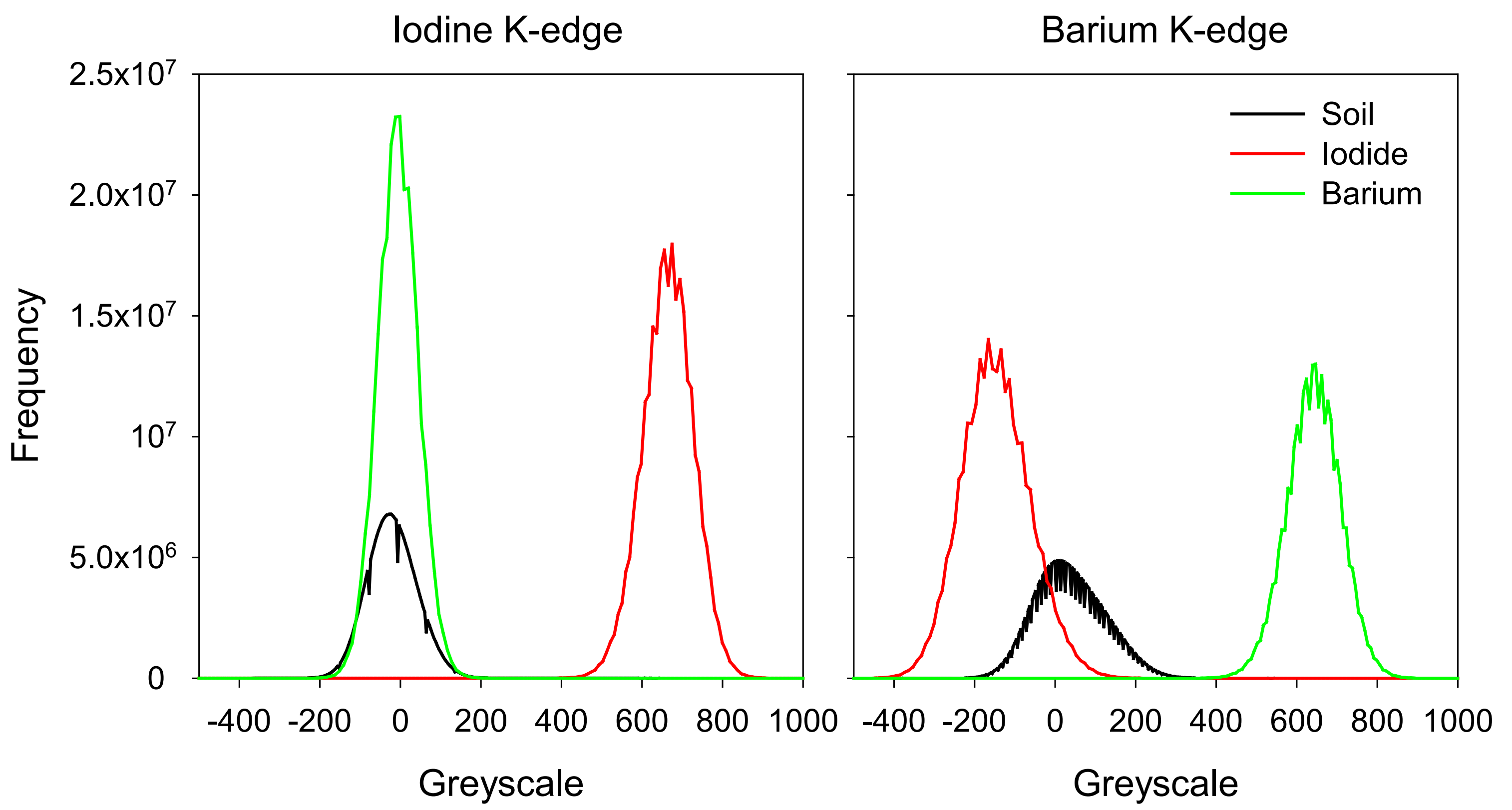

IV. Tests and validation

Soil aggregate fractions:

Small	< 0.05 mm
Medium	0.10 – 0.50 mm
Large	1.00 – 2.00 mm

Sample size: ID 8.6 mm
Scanning Resolution: 4 mm
Scanning energy: 33.269 and 33. 069 keV
Dopant: 10% KI solution

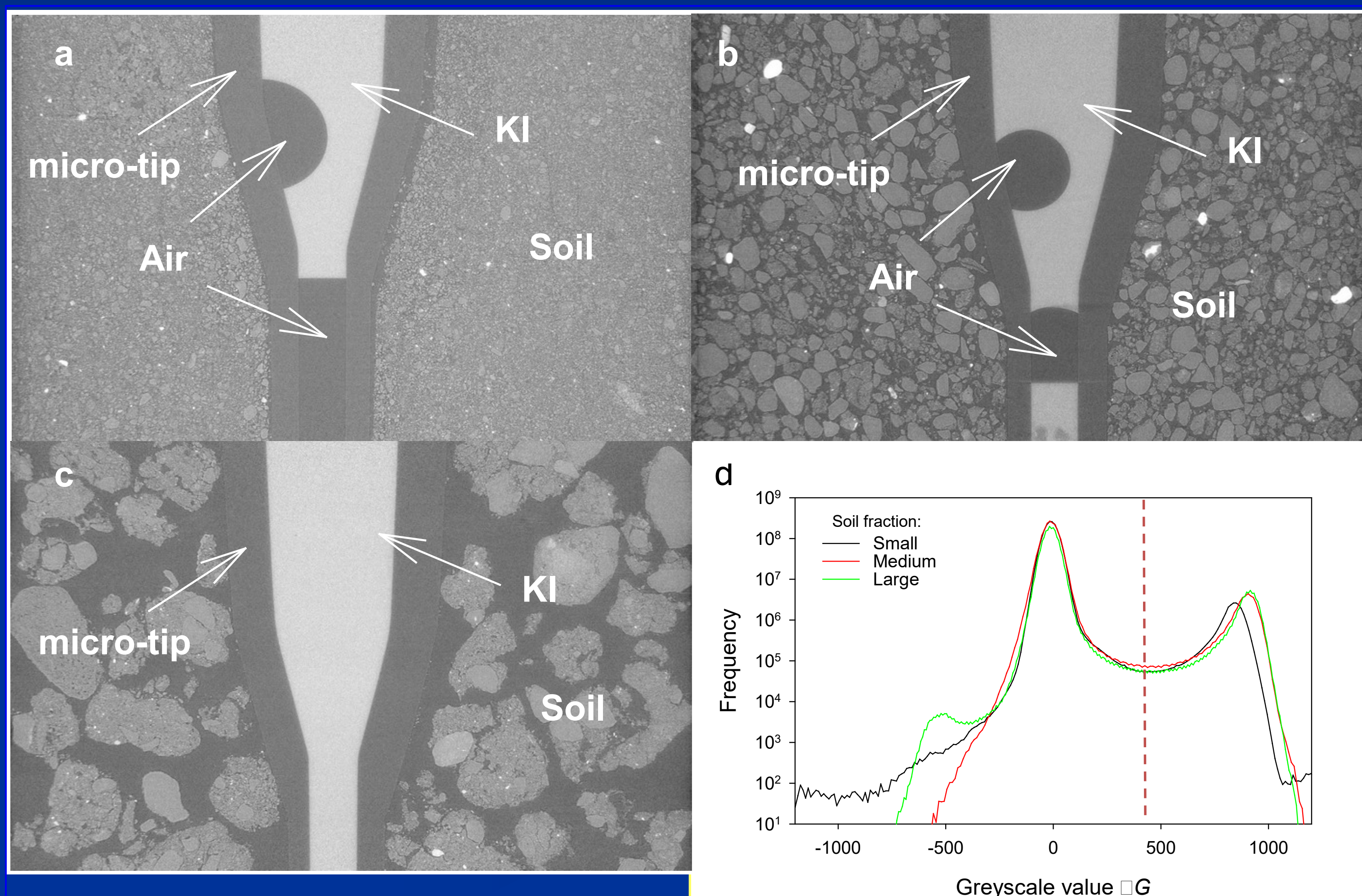

IV. Tests and validation

Theoretical relationships between Greyscale value and dopant concentration in solution

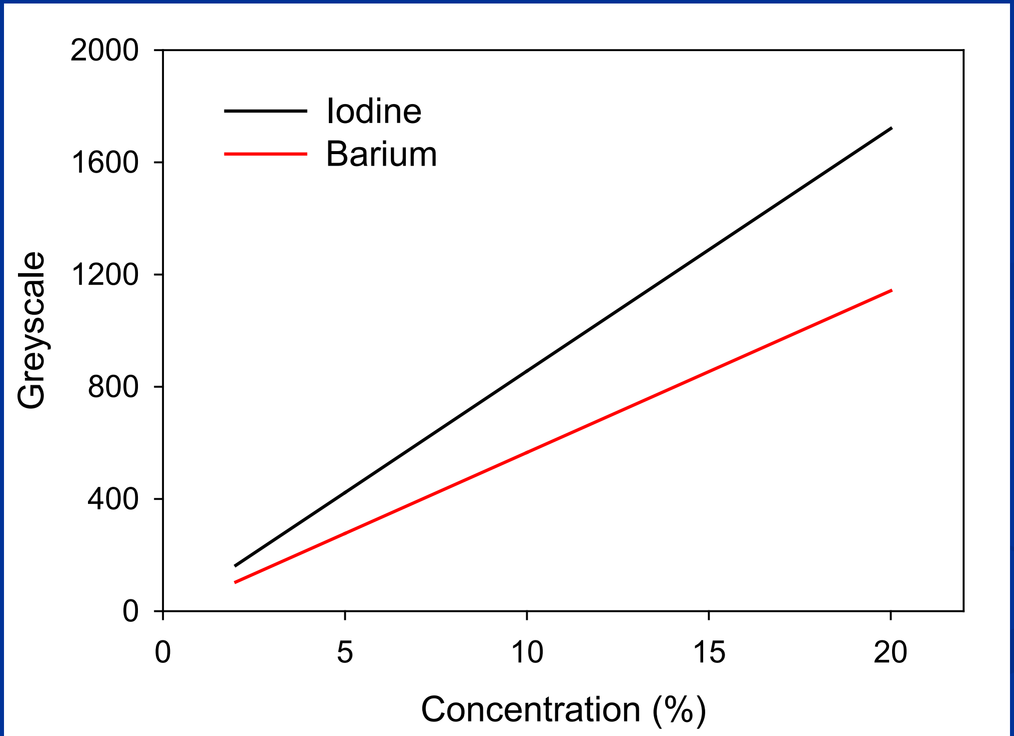

Effect of dopant concentration on the Greyscale histograms in two soil fractions

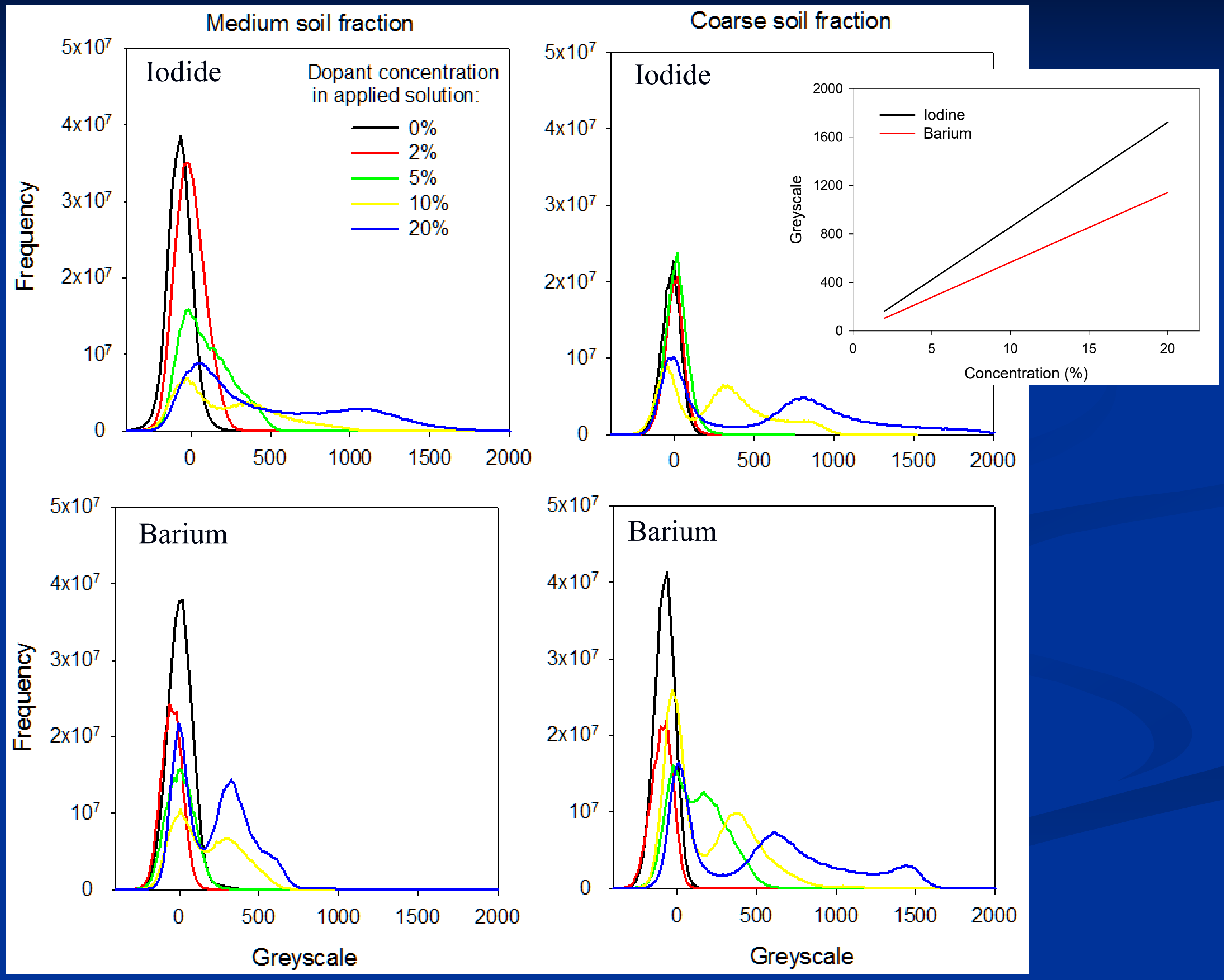

IV. Tests and validation

Soil aggregate fractions:	Small	< 0.05 mm
	Medium	0.10 – 0.50 mm
	Large	1.00 – 2.00 mm

Sample size: ID 8.6 mm
Scanning Resolution: 4 mm
Scanning energy: 33.269 and 33. 069 keV
KI contents: 0.1, 0.25, 0.4 $cm^3\ cm^{-3}$

G_a-G_b images for the 3 soil fractions after application of 10% KI solution (a-c) and a grayscale histograms for G_a-G_b image sequences (d). Brightness increases with an increase in iodide content.

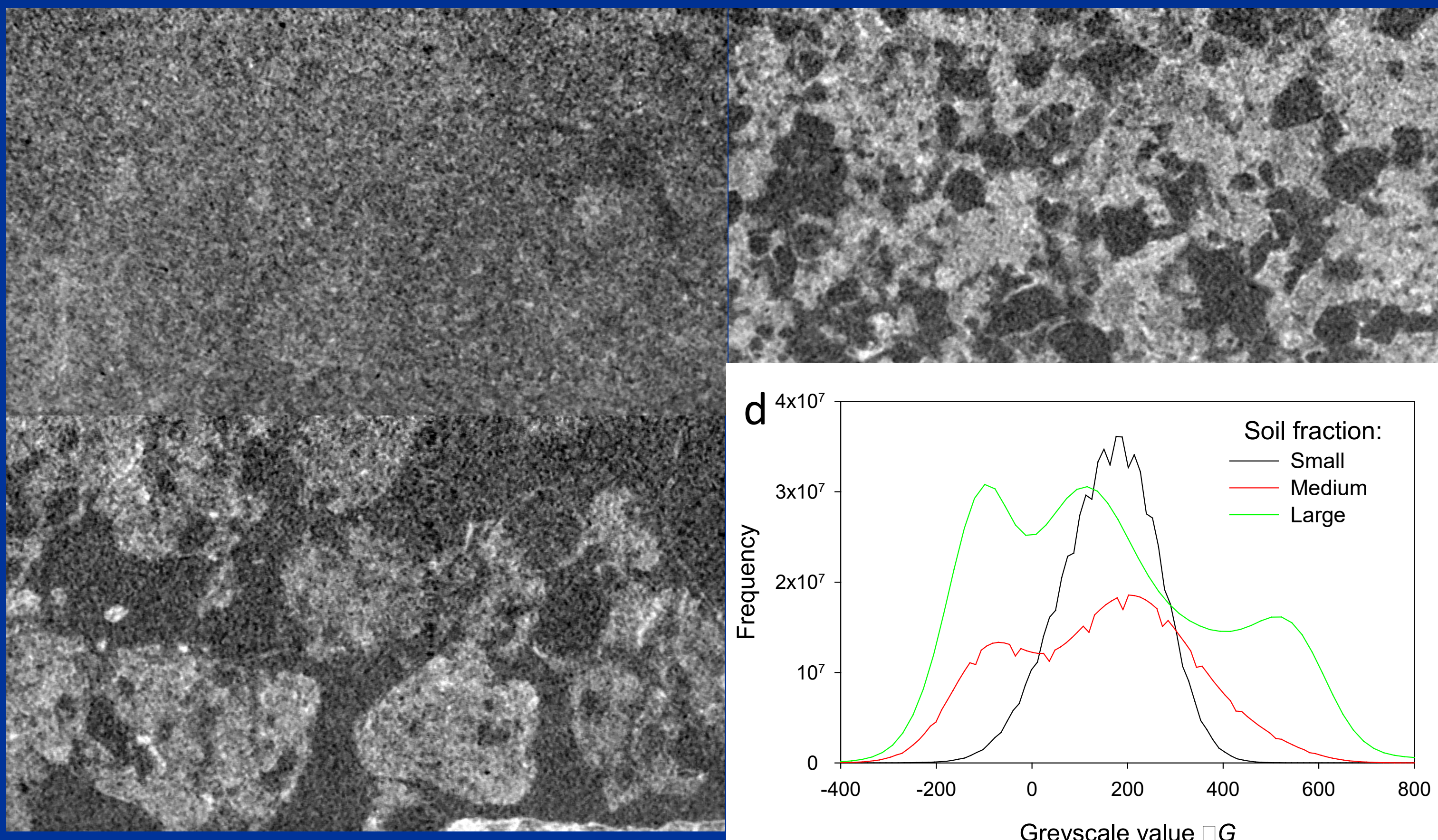

IV. Tests and validation

Iodide contents estimated in 3 soil fractions using the 16 standard thresholding methods and the new mass-balance approach.

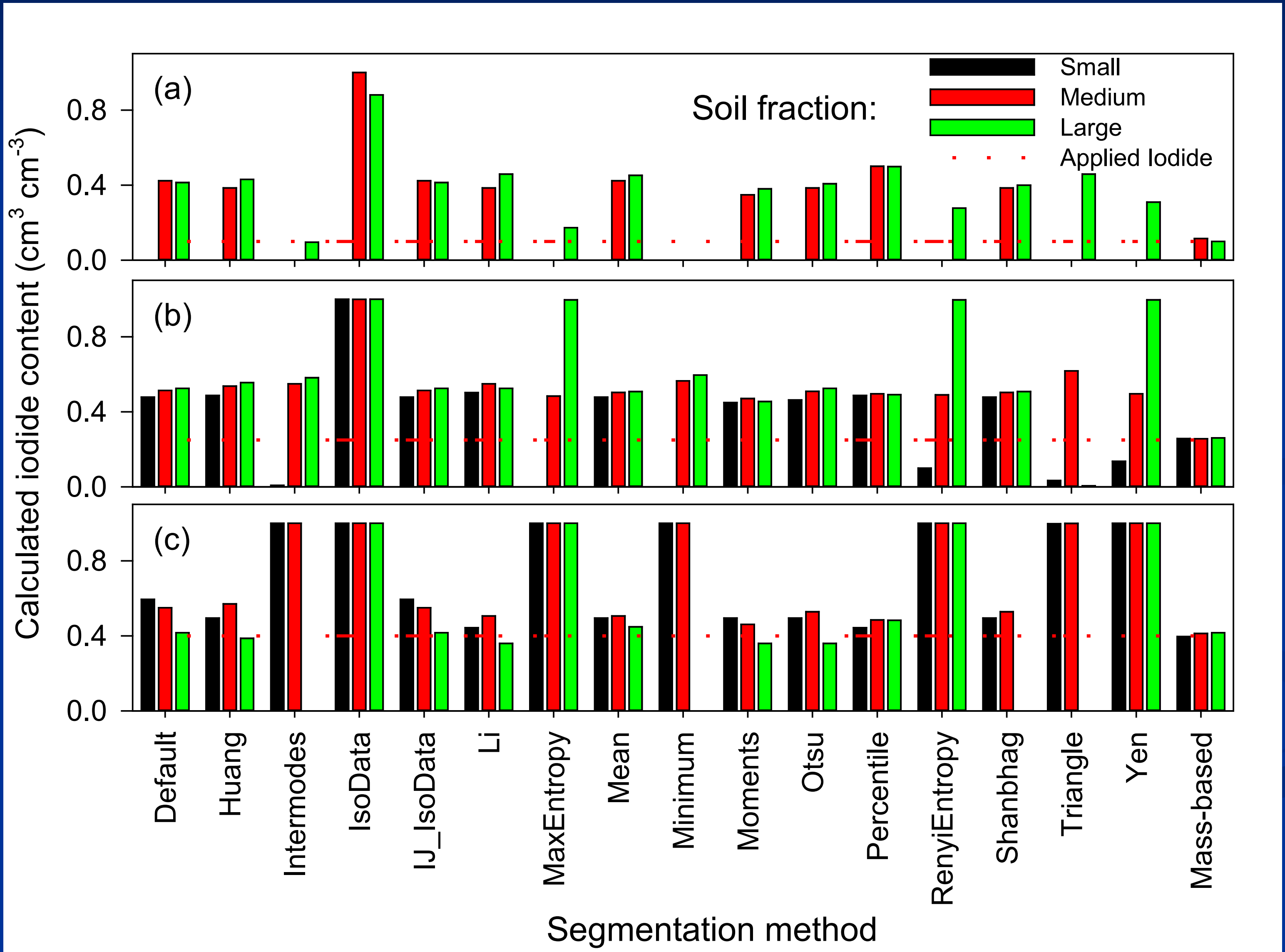

V. Applications

Distribution of water in the soil and in the plant leaf residue

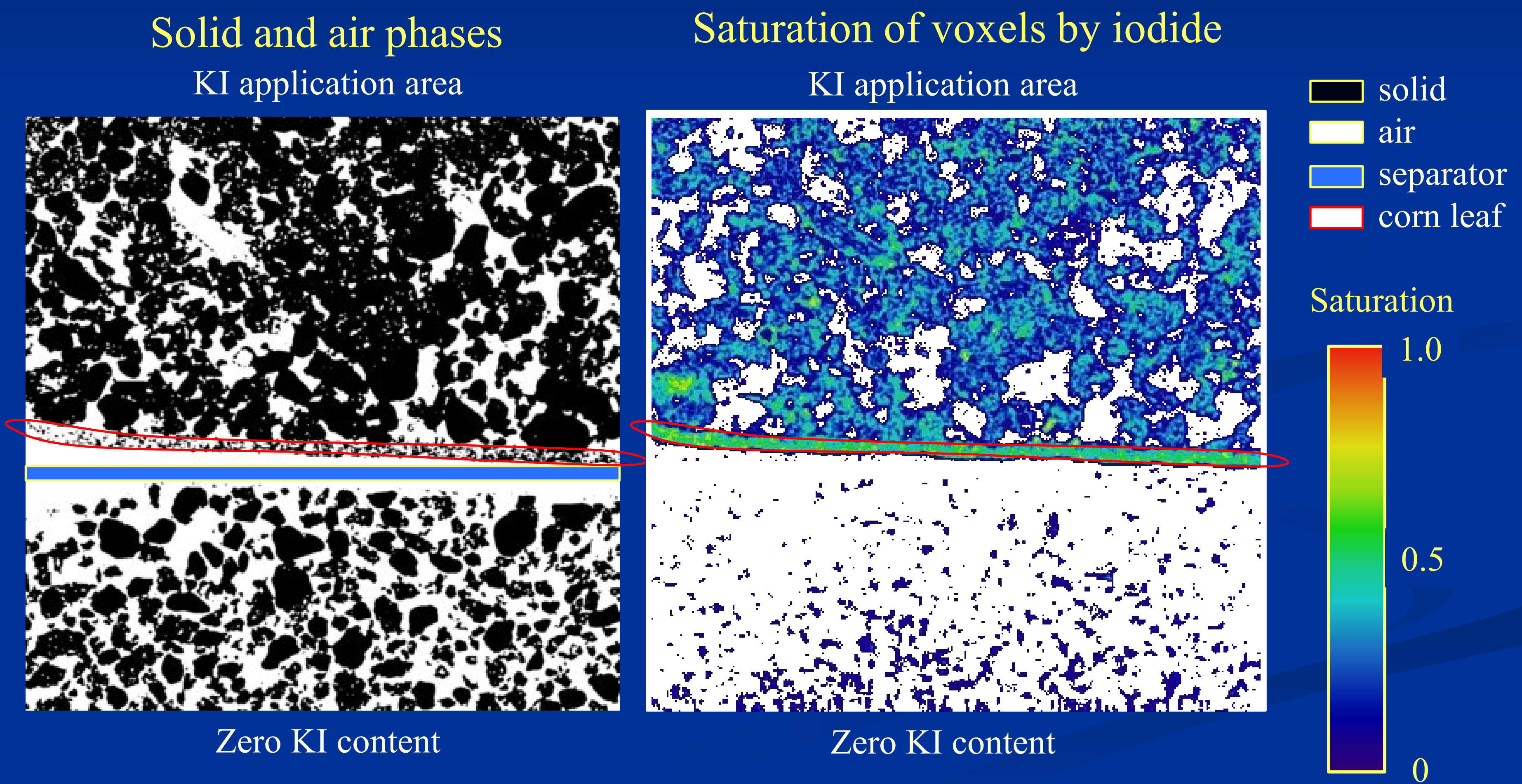

V. Applications

Visualization of the solution in a 0.1 – 0.5 mm soil fraction at different pressure heads

Iodide - 7 kPa Water - 4.6 kPa Barium - 1.5 kPa Air

solid
air

Solid and air phases

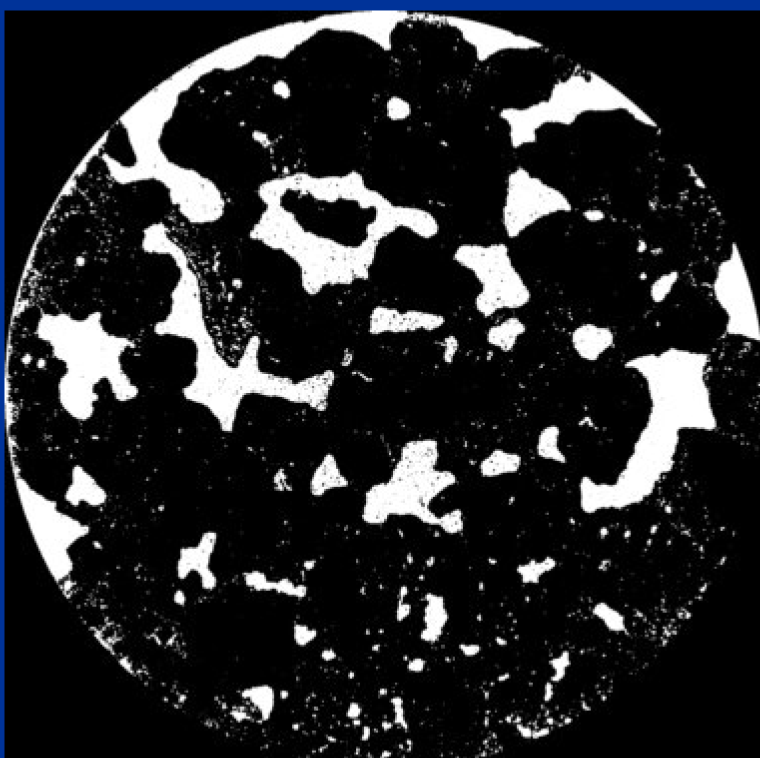

Saturation of voxels by iodide at -7 kPa

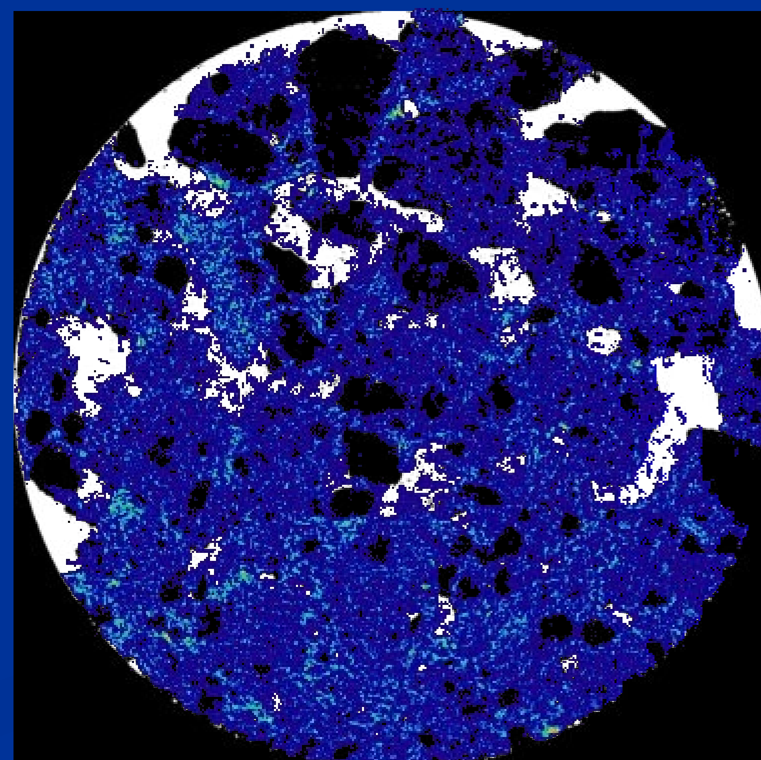

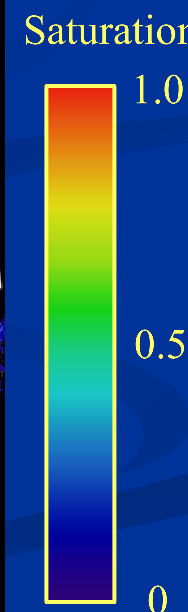

V. Applications

Visualization of the solution in a 0.1 – 0.5 mm soil fraction at different pressure heads

Iodide - 7 kPa Water - 4.6 kPa Barium - 1.5 kPa Air

Solid and air phases

Saturation of voxels by barium at -1.5 kPa

solid
air

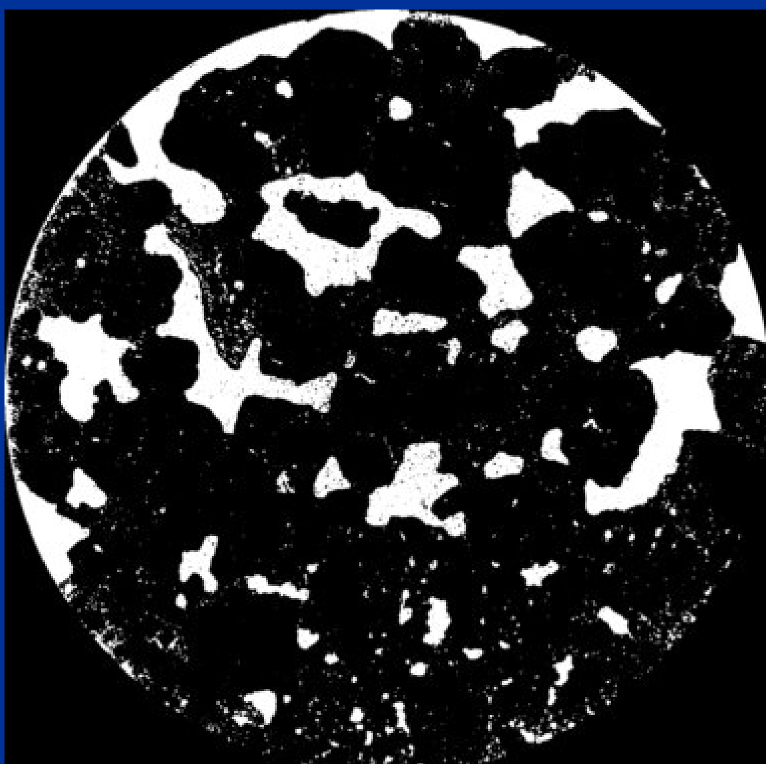

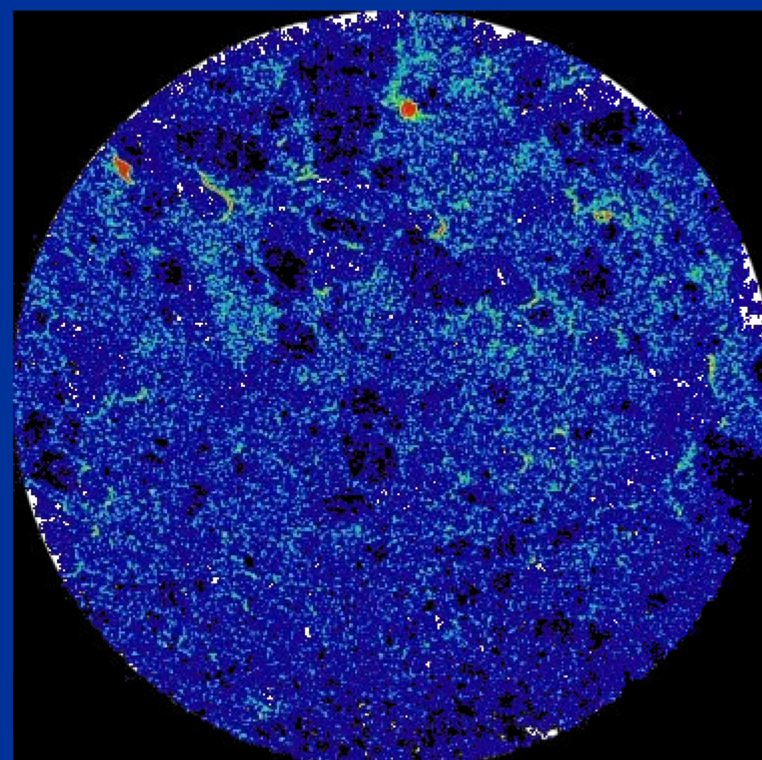

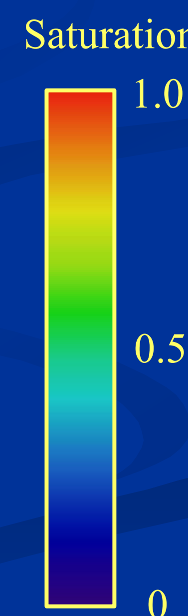

V. Applications

Visualization of the solution in an intact soil at different pressure heads

Iodide - 7 kPa Water - 4.6 kPa Barium - 1.5 kPa Air

Solid and air phases

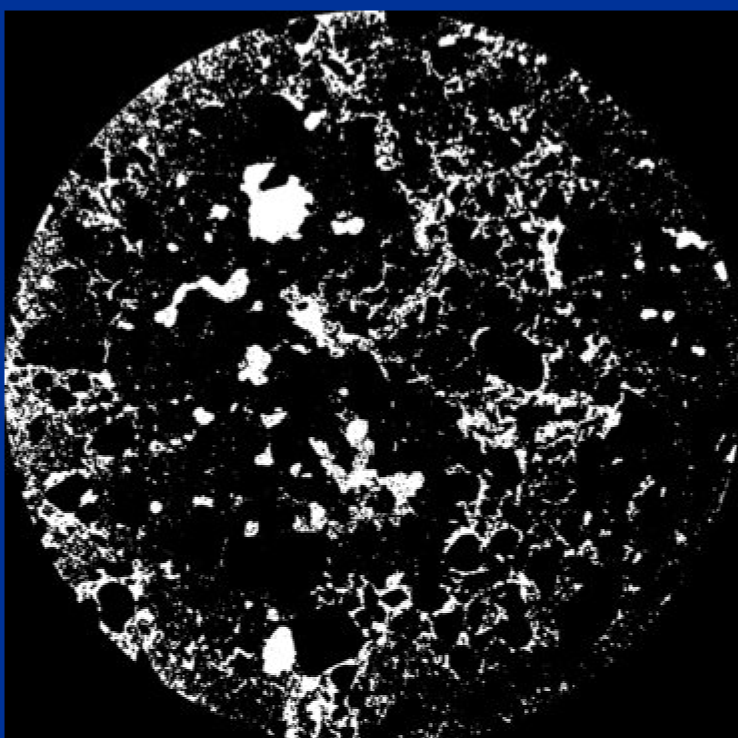

Saturation of voxels by iodide at -7 kPa

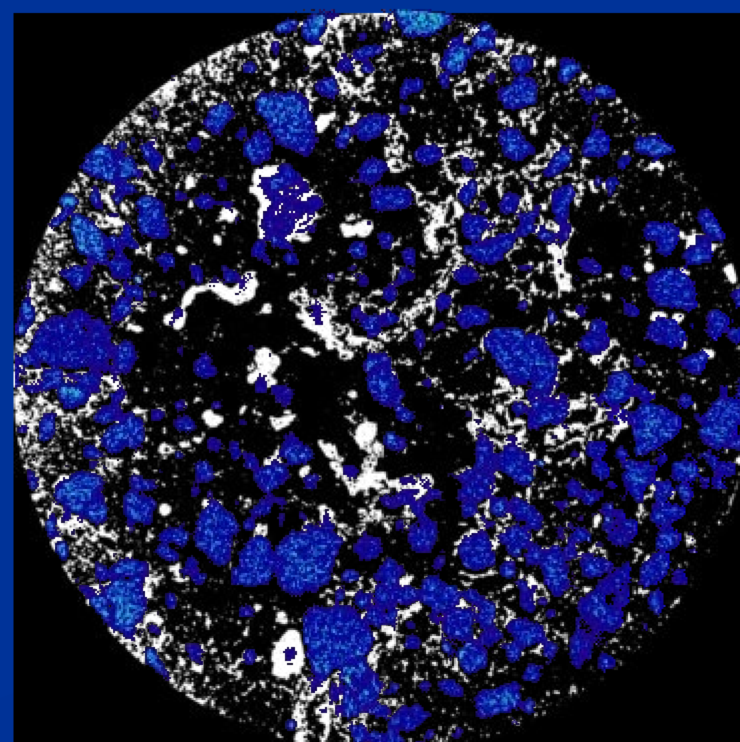

solid
air

Saturation

V. Applications

Visualization of the solution in an intact soil at different pressure heads

Iodide - 7 kPa Water - 4.6 kPa Barium - 1.5 kPa Air

Solid and air phases

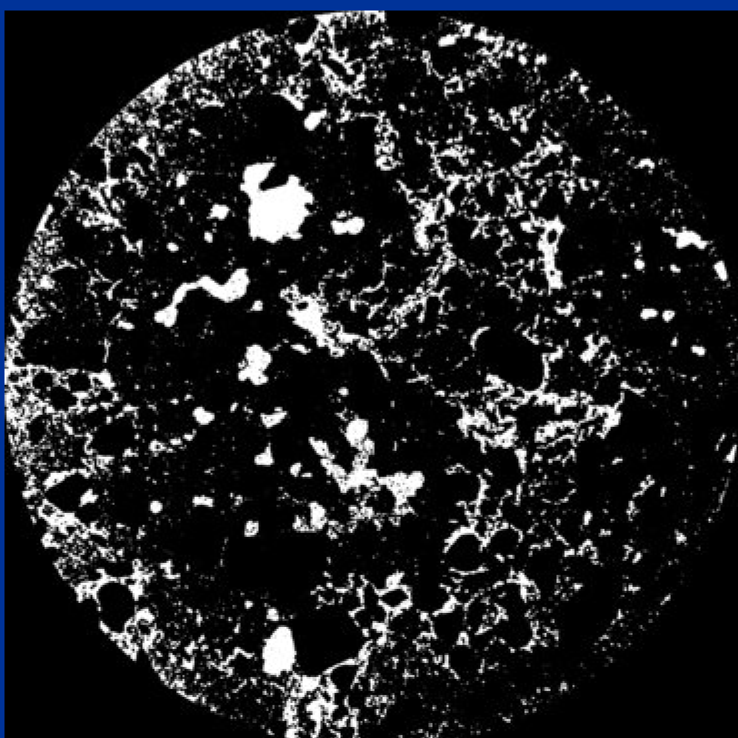

Saturation of voxels by barium at -1.5 kPa

solid
air

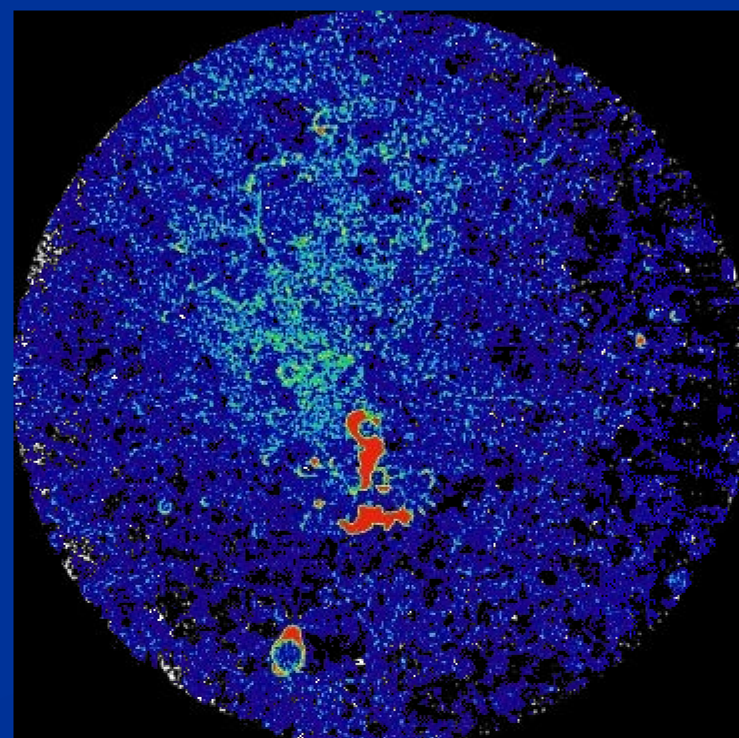

Saturation

Remarks

- All tested standard techniques of thresholding overestimated iodide content in the soil.

- The accuracy of the proposed mass-based approach was much higher as compared to that of the standard methods.

- The errors of estimating water distribution in soil using the balance methods can be caused by:
  1. a random noise of X-ray CT;
  2. uneven distribution of dopant in soil pores due to diffusion, anion exclusion, adsorption or mixable displacement of dopant in soil pores during its application.

- Developed method does not allow estimating fraction of solid and air in partly saturated soils, thus needs further development.

Thank you!

Acknowledgements: This work was funded in part by the National Science Foundation's Geobiology and Low Temperature Geochemistry Program (Award# 1630399). This material is partly based upon work supported by the U.S. Department of Energy, Office of Science, Office of Biological and Environmental Research under Award Number DE-SC0018409, and work funded by the DOE Great Lakes Bioenergy Research Center (DOE BER Office of Science DE-FC02-07ER64494). This research used resources of the Advanced Photon Source, a U.S. Department of Energy (DOE) Office of Science User Facility operated for the DOE Office of Science by Argonne National Laboratory under Contract No. DE-AC02-06CH11357. The authors would like to thank Dr. Mark Rivers (*Director, Center for Advanced Radiation Sources, ARGONNE National Lab.)* for help in X-ray CT imaging.